Applied Journal of Physical Science
Volume 3(4), pages 114-124, December 2021
Article Number: 7E24F1391
ISSN: 2756-6684
https://doi.org/10.31248/AJPS2021.058
https://integrityresjournals.org/journal/AJPS
Full Length Research

The connection between the critical frequency and the total electron content of the ionosphere at low and high solar activity period

Vivian Otugo[1,2]*, Charity Okujagu[2] and Sylvester Onwuneme[2]

[1]Department of Physics, University of Port Harcourt, Port Harcourt, Nigeria.
[2]Department of Physics, Rivers State University, Port Harcourt, Nigeria.

*Corresponding author. Email: vivian.akaogu@ust.edu.ng

Copyright © 2021 Otugo et al. This article remains permanently open access under the terms of the Creative Commons Attribution License 4.0, which permits unrestricted use, distribution, and reproduction in any medium, provided the original work is properly cited.

Received 8th September, 2021; Accepted 2nd October, 2021

ABSTRACT: Ionosonde-f_0F2 measurements and corresponding GNSS TEC measurements have been analysed. Available f_0F2 and TEC data respectively obtained from a pair of ionosonde and GNSS receiver stations of a mid-latitude station, named MO155, located in Moscow (55.8˚N, 37.2˚E), for 2010 and 2014 was used. Data for two years were respectively used in the study to represent years of low and high solar activity. A significant relation between the ionosonde-f_0F2 measurements and the corresponding GNSS-VTEC measurements with correlation coefficients above 0.8 was observed for both periods. The f_0F2/TEC ratios, for the MO155 station illustrated, are typically in the range of about 0.2 to 1.6 Mhz/TECU during the low solar activity period and 0.2 to 2.5 Mhz/TECU during the high solar activity period. The ratio is lower during the day-time, and higher during the nights and early mornings. The analysis of the four seasons for both periods (low solar activity and high solar activity) reveals a strong relationship between TEC and f_0F2 in all the seasons. Significantly, summer season appear to have a different trend from all other seasons with a relatively low correlation. The relationship between TEC and f_0F2 seem to be stronger during period of high solar activity than period of low solar activity. Results from the work indicate that the relationship between f_0F2 and TEC is mostly dependent on the seasons, followed by the level of solar activity, and then the local time. It was shown that the relationship between f_0F2 and TEC is not purely monotonic as suggested earlier; but that this relationship depends on factors like the season, level of solar activity, and local time. Considering the strong relationship between f_0F2 and TEC, the study affirms the method of using TEC as a proxy for f_0F2 estimation.

Keywords: f_0F2**,** TEC, ionosphere, seasons.

Key points

1. f_0F2 and TEC are found to highly correlated at both low and high solar activity period.
2. The relationship between f_0F2 and TEC is affected by seasons and solar activity.

INTRODUCTION

The ionosphere is a layer in the upper atmosphere is characterized by the presence of ionized plasma. The plasma is produced by a neutral atmospheric absorption of solar extreme UV and X- ray radiations (Cander, 1998). The ionosphere is located between the altitude of approximately 60 and 500 km. The ionosphere is subject to solar radiation and other factors such as solar winds, magnetic storm and earth's magnetism. These factors generate the ionization and photo-dissociation processes in the ionosphere.

The ionosphere disrupts the electromagnetic waves and in turn affect the precision of the results derived from the

Global Navigation Satellite System (GNSS) and that of radio communication (Mendoza et al., 2017). Due to the significance of the ionosphere and its temporal and spatial variability, researchers are continuously exploring this region. Moreover, since the ionosphere is mostly described by the values of its Total Electron Content (TEC) and by the critical frequency of the F2 layer (f_0F2), their measurements are needed. Fortunately, TEC measurements are easily accessible through GPS receivers at most locations. However, f_0F2 data are not available in most locations due the cost of ionosonde (the instrument for the measurement of f_0F2). Thus, many ionospheric researchers have devised an alternative method of generating f_0F2 data. One of the methods is by using TEC measurements to estimate the f_0F2 values (Otugo et al., 2019, Ssessanga et al., 2014). Significantly, it has been proven in the past that the two parameters are co-related, however, there has not been a standard model establishing their connection.

Spalla and Ciarolo (1994) proposed a very straight forward model, as described in equation (1).

$$(f_0F2)^2 = 3.51\,TEC \qquad (1)$$

The units of f_0F2 and TEC in equation (1) are respectively MHz and TECU (TEC units).

Where 1 TECU = 10^{16} electron per square meter.

However, this model can only give a coarse approximation of f_0F2 median values (Ssessanga et al., 2014). Maltseva (2016) suggested that the seasonal correlation coefficient between TEC and f_0F2 over high and low latitude is in the range of 0.7 to 1.0 and the two parameters are more correlated in winter than in Spring. Kouris et al. (2004) suggests that the daily variation of TEC and f_0F2 are similar for low and moderate solar activity periods. Not much research has been done on the relationship of these two parameters during periods of high solar activity. Studies in this aspect is quite important, since ionospheric variability is known to be relatively high during the period of high solar activity.

Therefore, this paper presents the empirical relationship between f_0F2 and TEC during periods of high solar activity using data from a mid-latitude station. It was demonstrated that the relation between f_0F2 and TEC is dependent on local time, seasons and solar activity.

LITERATURE REVIEW

Total Electron Content (TEC) and its measurements

The total electron content (TEC) of the earth's ionosphere is the total number of free electrons along a particular line of sight between the receiver and a GPS satellite in a column of 1 m^2 cross sectional area (Klobuchar, 1986 Ezquer et al., 2004). TEC is measured in electrons per square meter; where10^{16} electrons/m^2 is equal to 1 TEC unit (TECU) (Davies and Hartmann, 1997). It is a significant descriptive parameter in ionospheric studies (Fayose et al., 2012). TEC values are used in describing the F2 region at various locations even during magnetically disturbed periods. Any operating system that encompasses radio wave propagation through ionosphere needs TEC quantities; as TEC affects code signal transmission as well as the phase signal transmission observed in radio communication. In the times past, TEC measurements were carried out with Faraday Rotation effect on a linear polarized propagating plane wave. However, in the recent days, the use of GPS for TEC measurements has become predominant because GPS observation network has a widespread worldwide coverage.

To estimate the TEC values, a dual frequency GPS observation is mostly used. The dual frequency GPS data enhances the exactness of TEC values by eliminating the errors generated by ionospheric delay in signals. TEC is determined at different elevation angles from the slant angle; which gives the Slant Total Electron Content (STEC) and then transmitted to the vertical to generate the corresponding values of Vertical Total Electron Content (VTEC). The general relation for estimating STEC is given:

$$\int_S^R N_e ds_0 \qquad (2)$$

Where = *R* is the receiver, *S* is the satellite, N_e is the electron density and ds_o is the integration along the signal path from satellite to the receiver.

Correspondingly, VTEC can be obtained with the relation given by Klobuchar (1986):

$$V\,TEC = STEC \cos\left(sin^{-1}\left(\frac{ReCos\theta}{Re+h_{max}}\right)\right) \qquad (3)$$

Where: *Re* is the mean earth radius = 6378 km, h_{max} = 350 km; height of maximum electron density, θ is the angle of elevation at the ground station.

VTEC is used to map the TEC across the surface of the earth and by dividing it by the secant of the elevation angle at a mean ionospheric height of 350 to 450 km. (Ssessanga et al., 2014, Ya'acob et al., 2010).

Critical frequency of the F2 layer and its measurement

The critical frequency of the F2 layer (f_0F2) is one of the key parameters used in studying the ionosphere. The ionosphere may be described by different parameters, but the most widely used description of the ionosphere is the critical frequency (Mosna et al., 2008). This is because critical frequency is a well-defined parameter in radio communication. It gives the highest frequency at which radio signal may be reflected back to the earth by the F2 layer; and this information is needed by experts in radio communications to determine the value of frequency to use for a better transmission. The value of the f_0F2 is not steady; it varies with location, seasons, time of the day and other factors (Okoh et al., 2010; Mckinnell and Poole, 2004; Tshisaphungo et al., 2018). It varies throughout the year with season, with its maximum during summer (Wintoft and Cander, 2000). This implies that the instantaneous values of f_0F2 are required for a better radio transmission.

Ionosondes are used for the measurements of the f_0F2 and other ionospheric parameters. They are special types of radar used for studying and monitoring of the electron density at different heights of the ionosphere. Ionosonde generates accurate measurements of f_0F2 and operates on the principle of ionospheric plasma as a dispersive medium. A radio wave propagating into the ionospheric plasma has a refractive index, μ. In the absence of earth's magnetic field, the refractive index is given as (Reinisch et al., 2009):

$$\mu^2 = 1 - k({}^{N_e}/_{f^2}) \quad (4)$$

Where: *Ne* is the density of free electrons, *f* is the sounding frequency

and: $k = (e^2/4\pi\varepsilon_0 m) \approx 80.5$

Where, *e* = charge of electron, ε_0 = permittivity of free space and *m* = mass of electron.

Below the ionosphere, Ne = 0 and μ = 1; within the ionosphere, Ne > 0 and μ < 1

The sounder transmits radio signals vertically by scanning a large frequency band from about 1 to 30 MHz as to cover the ionization structure from the E-region to the F-region (Reinisch, 1986). At a level, when the critical frequency of the radio waves f_c becomes equal to plasma frequency f_p($f_c = f_p$), the refractive index μ becomes zero ($\mu \approx 0$). At this point, the radio wave cannot propagate further, but it is reflected, hence equation (4) is reduced to (Davies, 1990):

$$f_p^2 = k(N_e) \quad (5)$$

Correspondingly, the time τ, which is the time it takes for the radio signals to be reflected back to the receiver is recorded. By applying equation (4) and the recorded time τ, one can deduce the maximum electron density (N_m) and the altitude of reflection of the different layers of the ionosphere, hence generating the electron density profile (Ssessanga et al., 2014).

It is important to note that the maximum electron density of the F2 layer is measured at a critical frequency known as the f_0F2. Both parameters are related with this expression (Davies, 1990):

$$NmF2 = 1.24 \times 10^{10} \times f_0F2^2 \quad (6)$$

Where *Nm*F2 is the maximum electron density of the F2 layer.

METHODOLOGY

f_0F2 and TEC data were obtained from a pair of ionosonde and GNSS receiver station of a mid-latitude station; located in Moscow (55.8˚N, 37.2˚E). Ionosonde observations of f_0F2 values were obtained from the archives of the Space Physics Interactive Data Resources (SPIDR, http://spidr.ngdc.noaa.gov/spidr). The TEC measurements were obtained from a corresponding GNSS receiver station, from the data archives of the University of California, San Diego (www.garner.uscd.edu). The VTEC data were obtained in RINEX (Receiver Independent Exchange) format. RINEX is a data interchange format for raw satellite system data which allows a user to post process the received data to generate a better result. RINEX gives information measured by 2 or more receivers in a differential mode. These RINEX data files were post processed into TEC files using a GPS-TEC analysis application software developed by GopiSeemala (Seemala and Valladares, 2011) (available from https://seemala.blogspot.com). Typically, TEC are measured at an arbitrary slant ray paths between the satellite and receiver station. To convert these slant TEC to Vertical TEC, a thin shell model at the Ionospheric Pierce Point (IPP) height of 350 km (Rama Rao et al., 2006), was assumed (Mannucci et al., 1993; Langley, 2002); to rotate the actual slant measurement to the equivalent VTEC. Then, to obtain a 30-s instantaneous VTEC values for a receiver station, the average of all VTECs computed for satellites visible within the 30-s interval were computed. VTECs from satellites below 30-degree elevation angles were excluded from the computation so as to reduce multipath errors.

To further reduce the volume of data, smoothen out data spikes, and obtain VTEC values that correspond to the hourly f_0F2 values, the 30-s VTEC data were averaged in 1 hour interval. Furthermore, a MATLAB program was used to collate TEC data and the f_0F2 data together.

RESULTS AND DISCUSSION

Daily variation

The empirical relationship between f_0F2 and TEC was demonstrated. Different days in each of the four different seasons of the year were investigated. The year; 2010

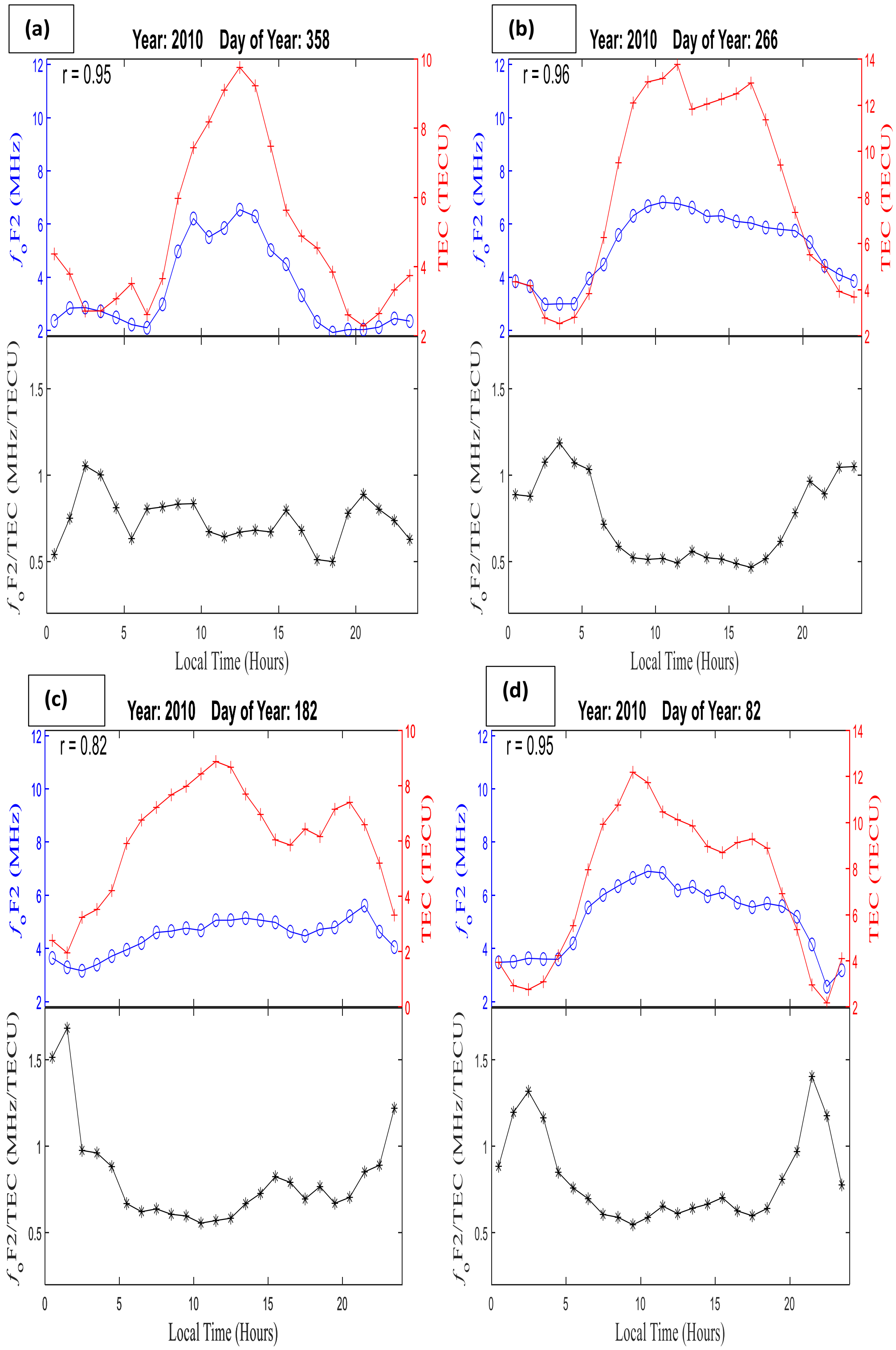

Figure 1. Daily Variation of TEC and f_0F2 during period low solar activity (a) Winter (b)Autumn(c) Summer and (d) Spring.

were chosen as period of low solar activity while 2014 were taken to represent period of high solar activity. The results of the diurnal profiles of ionosonde-f_0F2 and GNSS-VTEC was illustrated in Figures 1 and 2. The days illustrated were arbitrarily chosen to represent days in different seasons and different levels of solar activity. The bottom panels of the plots show corresponding diurnal profiles of the f_0F2/TEC ratio. The corresponding values of

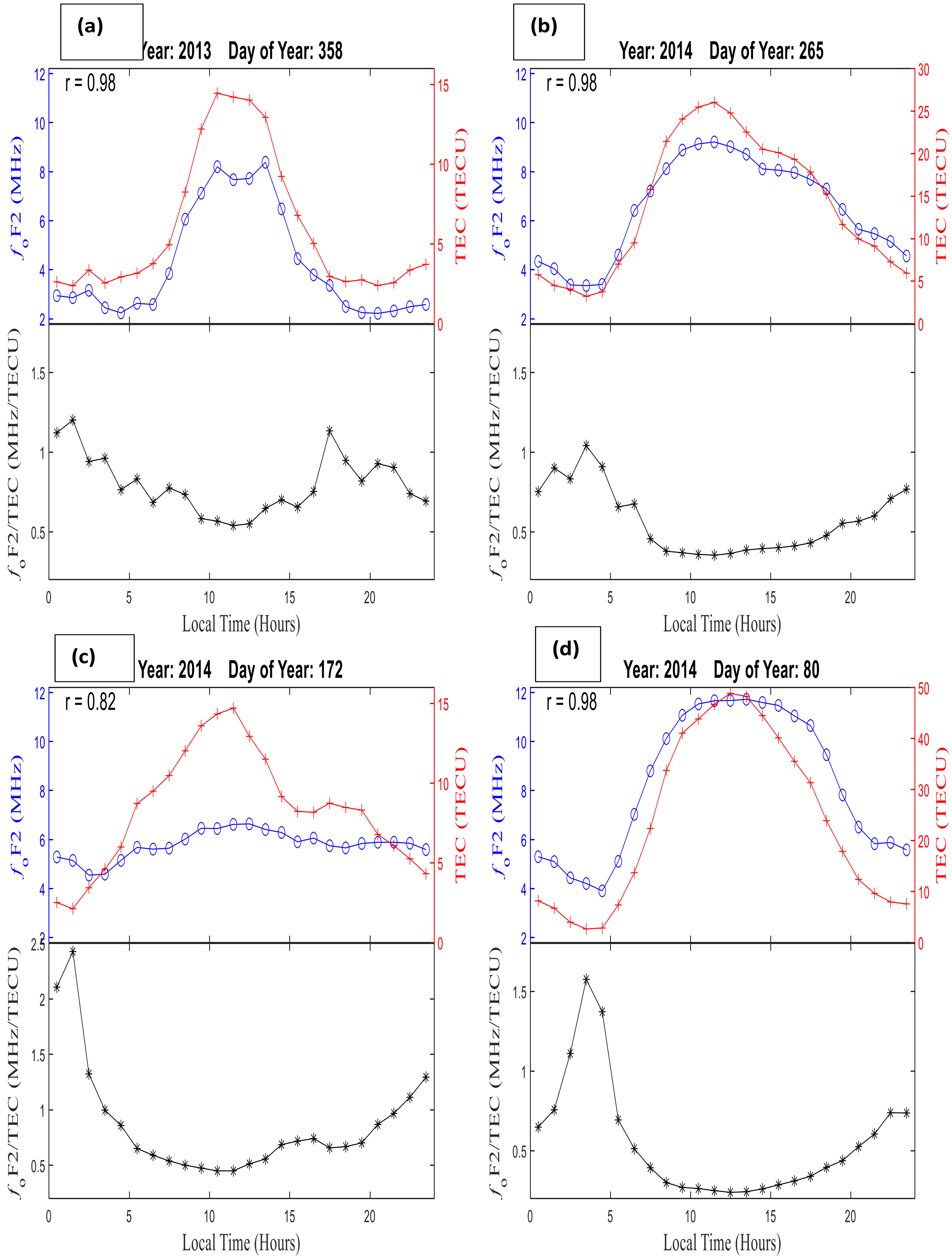

Figure 2. Daily Variation of TEC and f_0F2 during period high solar activity; (a) Winter (b)Autumn (c) Summer (d) Spring.

correlation coefficient (r) between the ionosonde-f_0F2 and GNSS-VTEC measurements were computed and are as shown on the plots.

In Figure 1, four different days from each of the four seasons of a low solar activity year (2010) was illustrated. The plot depicts clearly a very significant relation between the ionosonde-f_0F2 measurements and the corresponding GNSS-VTEC measurements. A very strong correlation of

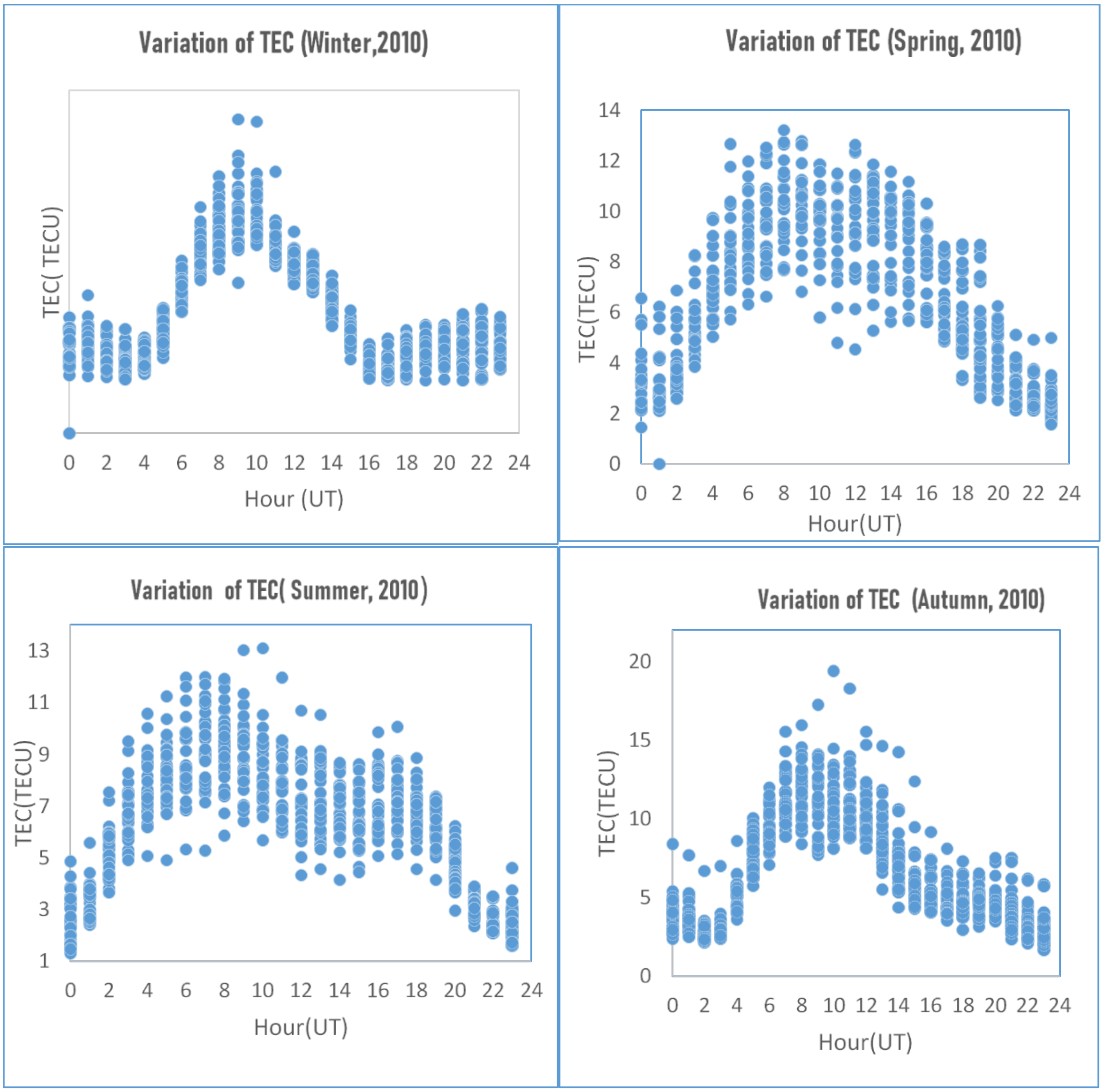

Figure 3. Seasonal variation of TEC during period of Low solar activity.

0.95, 0.96, and 0.95 was observed for the days in Winter, Autumn and Spring of 2010 respectively. The details are shown in Table 1. However, a slightly lower correlation of 0.82 was noticed during the summer. Figures 1(a) to (d) also show that the f_0F2/TEC ratio at low solar activity period are typically in the range of about 0.4 MHz/TECU to about 1.5 MHz/TECU. The ratio is lowest during the day-time (when the ionospheric ionization is high), and peaks at the early mornings (when the ionospheric ionization is low).

Correspondingly, the diurnal variation of TEC and f_0F2 values during the high solar activity period was also investigated. A very strong correlation of 0.98 was observed in 3 seasons (Winter, Autumn, Spring). Again, a relatively low correlation of 0.82; was observed during Summer. All the seasons show an observable peak around noon, but this is more pronounced during the Spring. The f_0F2/TEC ratio during this period are in the range of 0.2 to 2.5 Mhz/TECU.

Generally, the analysis of the daily variation of TEC and f_0F2 for all the seasons indicate that the quantity of f_0F2 and TEC in the ionosphere varies with local time. The values of both parameters builds up during the early hours of the morning and abruptly reaches its peak about noon, then decreases to a minimum around sunset. This variation in f_0F2 and TEC is as a result of strong photo-ionization during the day when there is high solar radiation; and the recombination during the night when there is little or no solar radiation. This finding is consistent with work done by Anderson and Fuller (1999). It has been observed that the F2 region contributes majorly to TEC during the daytime while at night-time, the plasmasphere

Table 1. Seasonal variation of TEC and f_0F2 values.

Season	Seasonal max		r (daily)	r (seasonal)
	TEC	f_0F2		
Low solar activity				
Spring	15.84	6.53	0.95	0.8
Summer	13.1	6.31	0.96	0.73
Autumn	19.43	8.94	0.82	0.87
Winter	12.83	7.31	0.95	0.84
High solar activity				
Spring	40.47	11.14	0.98	0.94
Summer	14.71	7.27	0.98	0.5
Autumn	43.23	12.36	0.82	0.97
Winter	27.57	10.99	0.98	0.98

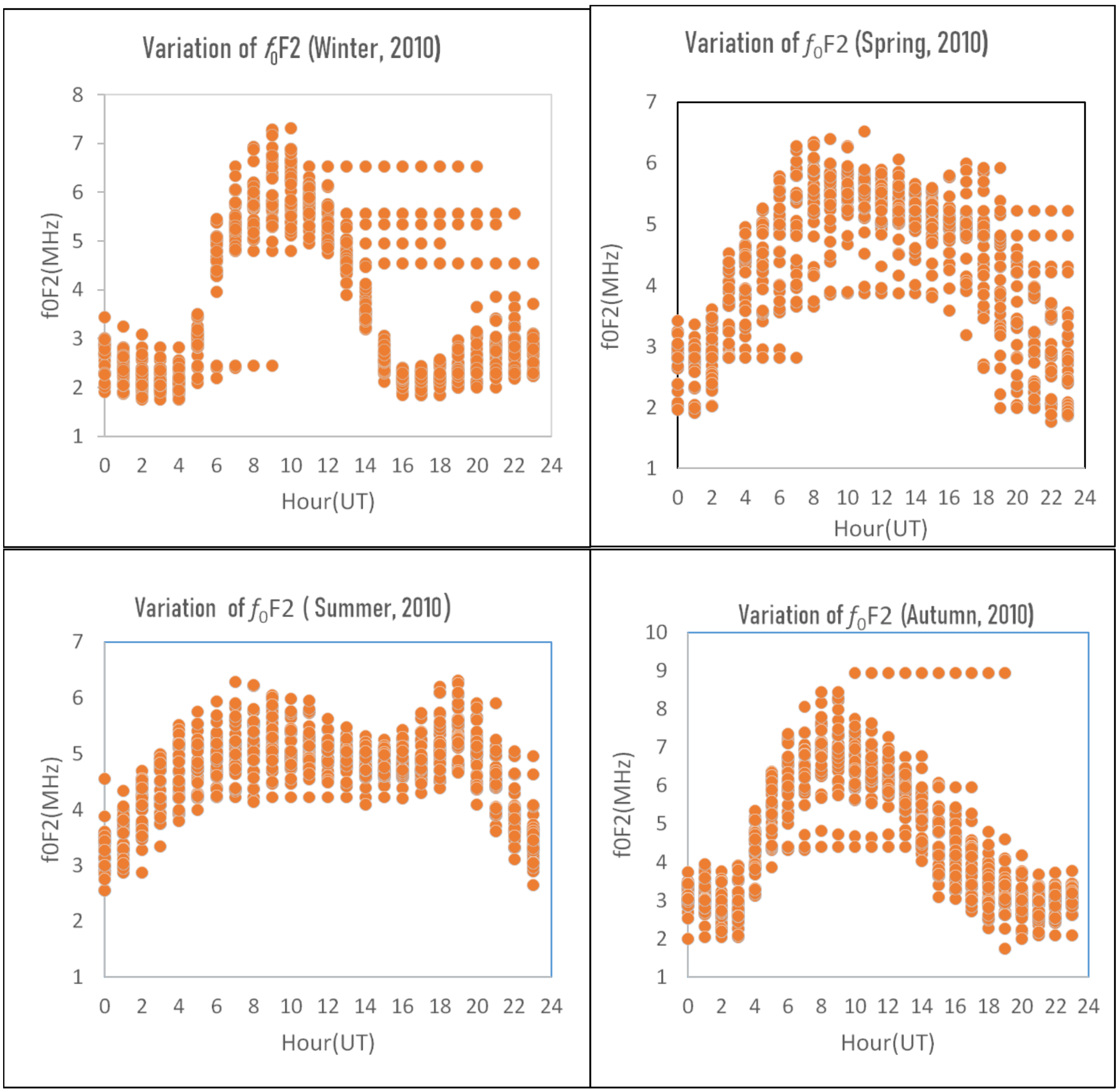

Figure 4. Seasonal variation of f_0F2 during period of Low solar activity.

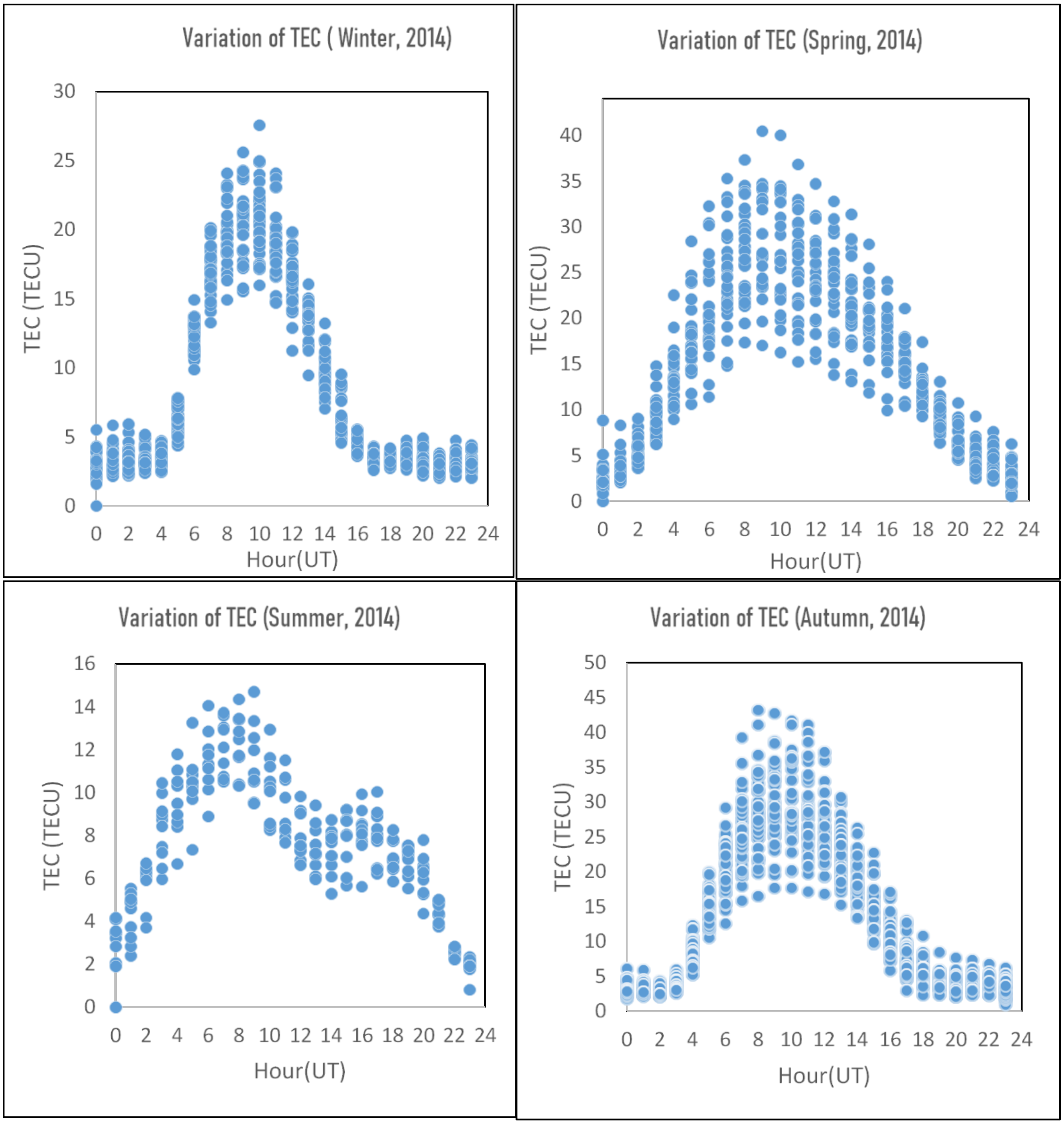

Figure 5. Seasonal variation of TEC during period of High solar activity.

does the major contribution; hence the correlation between f_0F2 and TEC decreases at night-time (Ssessanga et al., 2014; Klimenko et al., 2017). The result in this study confirms this assertion. Furthermore, one significant observation in the study is that the noon values of $f_0F2(N_mF2)$ are greater in Winter than in Summer (Winter anomaly).

Moreover, the results in this study clearly depict a very significant correlation between the ionosonde-f_0F2 measurements and the corresponding GNSS-TEC measurements for both periods. This is corroborated by the values of correlation coefficient which are generally greater than 0.9 for all illustrated cases except in summer where the correlation coefficient was slightly low.

Seasonal variation

An analysis of the effect of seasons on the relationship between TEC and f_0F2 at low and high solar activity period was done as well. The correlation coefficient between the two parameters in all the seasons was calculated; the results are displayed in Table 1. As observed in the daily variation, TEC and f_0F2 are strongly correlated in Winter, Autumn and Spring of low solar activity period with values above 0.8; with a relatively low value of 0.73 in Summer. Additionally, a scatter plot presented in this study illustrated how these parameters vary in each of seasons during the low solar activity period (Figures 3 and 4). The results show that in Winter, TEC and f_0F2 has a pronounced peak

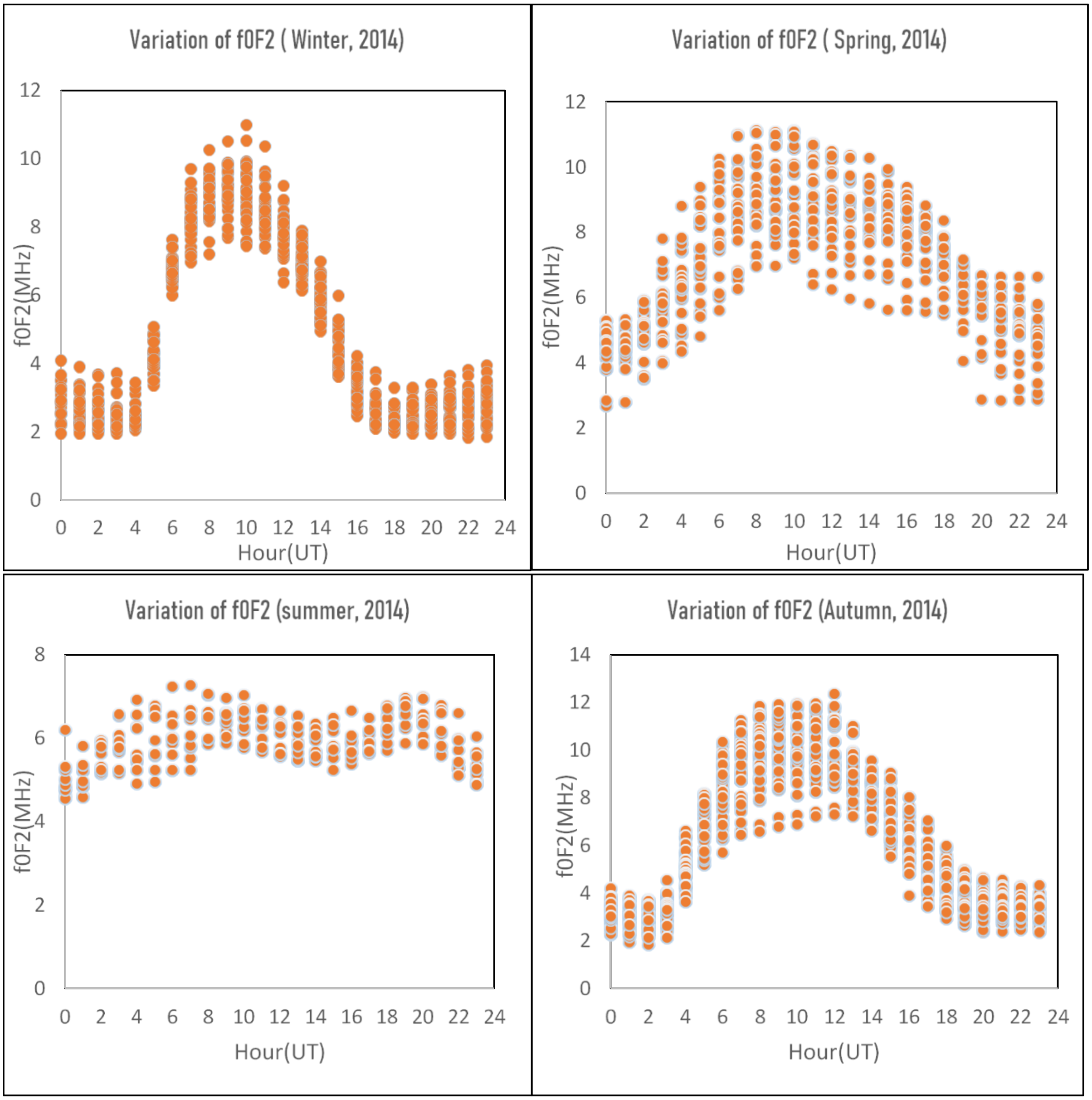

Figure 6. Seasonal variation of f_0F2 during period of High solar activity.

values between the hours of 10 and 12 noon LT with the minimum values at the early hours of the morning. This trend is also observed in Spring and Autumn. However, during the summer; TEC and f_0F2 values have their maximum values between 6.00 and 8.00 LT. The observation in this study is in line with Jenan et al. (2020); which observed that the daily peak of TEC is slightly delayed in winter than in summer.

In the investigation of the effect of seasons on the relationship between TEC and f_0F2 at high solar activity period, no significant difference was observed in the trend except that the amount of TEC and f_0F2 are much higher. This is shown in Figures 5 and 6. The increase in their amount is expected since there is increased ionization during this period. The correlation coefficient between TEC and f_0F2 during the high solar activity period is observed to be stronger than at low solar activity period (Table 1). Yet again, a very low correlation coefficient of 0.5 was observed during the Summer. Moreover, the maximum values of TEC and f_0F2 were found to be lower in summer when compared to other seasons. These findings are consistent with the work of Hajra et al. (2016) and Ogwala et al. (2019).

Conclusion

An empirical relationship between ionosonde-f_0F2 ments and corresponding GNSS TEC measurements has been analysed. Available f_0F2 and TEC data obtained from a pair of ionosonde and GNSS receiver station of a mid-latitude station; located in Moscow (55.8˚N, 37.2˚E), for 2010 and 2013 and 2014 was used.

A significant relation between the ionosonde-f_0F2 measurements and the corresponding GNSS-VTEC measurements with correlation coefficients of above 0.8 was observed. The f_0F2/TEC ratios, for the MO155 station illustrated, are typically in the range of about 0.2 to 1.6 MHz/TECU at low solar activity period and about 0.2 to 2.5 MHz/TECU at high solar activity period. The ratio is lower during the day-time, and higher during the nights and early mornings. Significantly, the findings reveal that TEC and f_0F2 are more correlated in other seasons (winter, Autumn and Spring) than in summer. Moreover, the maximum values of TEC and f_0F2 were found to be lower in summer when compared to other seasons. Also, the correlation of TEC and f_0F2 appear to be stronger during period of high solar activity than period of low solar activity.

Moreover, the results from the study demonstrated that the relationship between f_0F2 and TEC is not purely monotonic but that this relationship depends on factors like the season, level of solar activity, and local time. Considering the strong relationship existing between f_0F2 and TEC, the study affirms the method of using TEC as a proxy for f_0F2 estimation in cases where ionosondes are not available.

CONFLICTS OF INTEREST

The authors declare that they have no conflicts of interest.

ACKNOWLEDGEMENT

This research was supported by the University Support Program (USP) of the Centre for Atmospheric Research (CAR), National Space Research and Development Agency, Nigeria. We thank the Space Physics Interactive Data Resources (SPIDR) from which we obtained ionosonde data. Thanks to Boston College and Dr. Gopi Seemala for providing us with the GPS-TEC analysis application software used in this work.

REFERENCES

Cander, L. R. (1998). Artificial neural network application in ionospheric studies. *Annals of Geophysics,* 41(5-6), 757-766.

Davies, K. (1990) Ionospheric Radio. Peter Peregrinus Ltd., London.

Davies, K., & Hartmann G. (1997). Studying the Ionosphere with global positioning system. *Radio Science*, 32(4), 1695-1703.

Ezquer, R., Brunini, C., Mosert, M., Meza, A., Oviedo, R., Kiorcheff, E. & Radicella. S. (2004). GPS–VTEC measurements and IRI predictions in the South American sector. *Advances in Space Research*, 34(9), 2035-2043.

Fayose, R. S., Babatunde, R., Oladosu, O., & Groves, K. (2012). Variation of Total Electron Content [TEC] and their effect on GNSS over Akure, Nigeria. *Applied Physics Research*, 4(2), 105-109.

Hajra, R., Chakraborty, S. K., Tsurutani, B. T., DasGupta, A., Echer, E., Brum, C. G., Gonzalez, W. D., & Sobral, J. H. A. (2016). An empirical model of ionospheric total electron content (TEC) near the crest of the equatorial ionization anomaly (EIA). *Journal of Space Weather and Space Climate*, *6*, A29.

Jenan, R., Dammalage, T. L., & Panda, S. K. (2021). Ionospheric total electron content response to September-2017 geomagnetic storm and December-2019 annular solar eclipse over Sri Lankan region. *Acta Astronautica*, 180, 575-587.

Klimenko, M. V., Klimenko, V. V., Zakharenkova, I. E., Ratovsky, K. G., Korenkova, N.A., Yasynkevich, Y. V., Mylnikova, A. A., & Cherniak, I. V. (2017). Similarity and differences in morphology and mechanisms of the f0F2 and TEC disturbances during the geomagnetic storms on 26–30 September 2011. *Annals of Geophysics*, 35, 923-938.

Klobuchar, J. A. (1987). Ionospheric time-delay algorithm for single-frequency GPS users. *IEEE Transactions on aerospace and electronic systems*, 23(3), 325-331.

Kouris, S. S., Xenos, T. D., Polimeris, K. V., & Stergiou, D. (2004). TEC and foF2 variations: preliminary results. *Annals of Geophysics*, 47(4), 1325- 1332.

Langley, R. (2002). Mapping the low-latitude ionosphere with GPS, *GPS World,* 13(2), 41-47.

Maltseva, O., & Mozhaeva, N. (2016). The use of the total electron content measured by navigation satellites to estimate ionospheric conditions. *International Journal of Navigation and Observation*, Volume 2016, Article ID 7016208.

Mannucci, A. J., Wilson, B. D., & Edwards, C. D. (1993). A new method for monitoring the Earth's ionospheric total electron content using the GPS global network. *Proceedings of the 6th International Technical Meeting of the Satellite Division of the Institute of Navigation (ION GPS 1993),* pp. 1323-1332, Salt Lake City, UT.

McKinnell, L. A., & Poole, A. W. (2004). Neural network-based ionospheric modelling over the South African region. *South African Journal of Science*, 100(11), 519-523.

Mendoza, B., Ruiz, J., & Jaramillo, P. (2017). Implementation of an Electronic Ionosonde to Monitor the Earth's Ionosphere via a Projected Column through USRP. *Sensors*, 17(5), Article Number 946.

Mosna, Z., Šauli, P., & Santolık, O. (2008). Analysis of critical frequencies in the ionosphere. *WDS' Proceedings of Contributed Papers*. Pp.172-177.

Ogwala, A, Somoye, E., Ogunmodimu, O., Adeniji-Adele, R., Onori, A and Oyedokun, O. (2019). Diurnal, seasonal and solar cycle variation in total electron content and comparison with IRI-2016 model at Birnin Kebbi. *Annals of Geophysics*, 37, 775-789.

Okoh, D. I., McKinnell, L. A., & Cilliers, P. J. (2010). Developing an ionospheric map for South Africa. *Annales Geophysicae,* 28(7), 1431-1439.

Otugo, V., Okoh, D., Okujagu, C., Onwuneme, S., Rabiu, B., Uwamahoro, J., Habarulema, J. B., Tshisaphungo, M., & Ssessanga, N. (2019). Estimation of ionospheric critical plasma frequencies from GNSS-TEC measurements using artificial neural networks. *Space Weather*, *17*(8), 1329-1340.

Rama Rao, P. R., Niranjan, K., Prasad, D., Krishna, S. G., & Uma, G. (2006). On the validity of the ionospheric pierce point IPP altitude of 350 km in the Indian equatorial and low-latitude sector. *Annales Geophysicae,* 24*(8),* 2159-2168.

Reinisch, B. W. (1986). New techniques in ground-based ionospheric sounding and studies. *Radio Science*, 21(3), 331-341.

Reinisch, B. W., Galkin, I. A., Khmyrov, G. M., Kozlov, A. V., Bibl, K., Lisysyan, I. A., Cheney, G. P., Huang, X., Kitrosser, D. F., Paznukhov, V. V., Luo, Y., Jones, W., Stelmash, S., Hamel, R., & Grochmal, J. (2009). New Digisonde for research and monitoring applications. *Radio Science*, 44(1), RS0A24.

Seemala, G. K., & Valladares, C. E. (2011). Statistics of total electron content depletions observed over the South American continent for the year 2008. *Radio Science*, 46(5), RS5019.

Ssessanga, N., Mckinnell, L. A., & Habarulema, J. B. (2014). Estimation of f_0F2 from GPS TEC over the South African region. *Journal of Atmospheric and Solar-Terrestrial Physics*, 112, 20-30.

Spalla, P., & Ciraolo, L. (1994). TEC and f_0F2 comparison. *Annals of Geophysics,* 37(5), 929-938.

Tshisaphungo, M., Habarulema, J. B., & McKinnell, L. A. (2018). Modeling ionospheric f_0F2 response during geomagnetic storms using neural network and linear regression techniques. *Advances in Space Research*, 61(12), 2891-2903.

Wintoft, P., & Cander, L. R (2000). Twenty-four-hour prediction of f_0F2 using time delay neural networks. *Radio Science,* 35(2), 395-408.

Ya'acob, N., Abdullah, M., & Ismail, M. (2010). GPS Total Electron Content (TEC) prediction at ionosphere layer over the equatorial region. *Trends in Telecommunications Technologies*. Retrieved from https://www.intechopen.com/chapters/9691.